The mean lateral density distribution of muons in extensive air showers detected at Haverah Park

1974 J. Phys. A: Math. Nucl. Gen. 7 2041

(http://iopscience.iop.org/0301-0015/7/16/008)

J. Phys. A: Math., Nucl. Gen., Vol. 7, No. 16, 1974. Printed in Great Britain.

The mean lateral density distribution of muons in extensive air showers detected at Haverah Park

M L Armitage†, P R Blake and W F Nash

Department of Physics, University of Nottingham, Nottingham NG7 2RD, UK

Received 9 May 1974

Abstract. This paper presents the results and conclusions from an experiment carried out between 1969 and 1973 at the Haverah Park cosmic ray extensive air shower detector array near Harrogate, Yorkshire. The detector consisted of 12 m^2 of shielded neon flash tubes sensitive to muons of energy greater than 300 $\sec\theta$ MeV.

The detector was situated at the centre of the EAS array and its response to showers of primary energy 10^{17} eV $\lesssim E_p \lesssim 10^{19}$ eV, with zenith angles up to 60° has been studied. The analysis has been restricted to those showers in which the distance (R) from the core of the shower to the detector was in the interval 100 m $< R <$ 1000 m. The results are compared with model calculations and a number of conclusions drawn.

1. Introduction

The long interaction mean free path of muons enables studies of the muon component of extensive air showers (EAS) at sea level to yield information concerning the interactions high in the atmosphere in which their parent pions are produced. The lateral spread of a muon away from the centre of the EAS is primarily due to the height of the interaction in which the pion is produced and the transverse momentum given to the pion. Hence the muon component of an EAS contains information concerning both the form of the nuclear interactions taking place and the longitudinal development of the EAS through the atmosphere. This development is dependent to some extent upon the mass of the primary cosmic ray initiating the shower.

The Haverah Park EAS installation consists of an array of deep water Čerenkov detectors spread over an area of about 12 km^2. A full description of the array is given by Wilson (1969). The deep water Čerenkov detectors measure the energy lost by the shower particles in traversing 1·2 m of water. The array detects EAS of energy 10^{17}–10^{20} eV with zenith angles less than 60° and core distances from the centre of the array of up to 2 km.

The parameter used as the measure of EAS size at Haverah Park is ρ_{500}. This is the energy loss density assigned to an EAS in traversing a slab of water, 1·2 m thick, at a distance of 500 m from its axis. The magnitude of this parameter has been shown to be largely insensitive to fluctuations in shower development and also only very weakly dependent on the details of the nuclear interactions and the primary mass. The energy of the primary particle therefore appears to be the dominant contribution to the value of ρ_{500}. Furthermore, for showers which lie within the perimeter of an EAS array, there

† Now at Computing Laboratory, University of Salford.

is generally a distance at which analysis of the same experimental data using different assumed lateral density distribution functions predicts the same density at that distance. This distance is characteristic of the array spacing and at Haverah Park is approximately 500 m. The shower size parameter ρ_{500} is therefore preferred to more conventional parameters.

The data presented here deal with the mean density distributions of the muon component in EAS. The accurate determination of these mean characteristics is essential before useful studies can be undertaken upon the fluctuations observed between showers.

2. The muon detector

The detector consists of three almost identical stacks of neon flash tubes and lead absorber as shown in figure 1. The total effective area is 12·4 m^2. The sides of the flash-tube stacks are shielded by 15 cm thick lead walls and the ends of the flash tubes are 30 cm in from the end of the shielding.

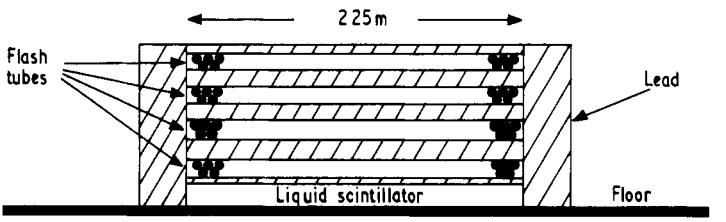

Figure 1. Scale drawing of side view of muon detector.

The flash tubes (2 m × 1·74 cm) are arranged in trays of two layers with electrodes between each layer. The total thickness of the absorber in the vertical direction is 15 cm of lead and 7·5 cm of steel, corresponding to an estimated muon detection threshold energy of 288 MeV. The multilayer nature of the absorber enables knock-on electrons produced in the lead to be identified.

The application of the high voltage pulse to the flash tubes occurs 13·6 μs after the reception of the EAS trigger pulse from the Haverah Park array. This delay has been found necessary to enable the records of other experiments to be completed before the spark gaps are triggered. With this delay the individual layer efficiency of the flash tubes (with respect to recording EAS shower particles at the Haverah Park trigger frequency of about 30/day) is 77·5%. This efficiency was calculated by selecting single muons in near vertical EAS.

From the film record, a track is classified as a muon if at least one tube flashed along the trajectory in three of the four trays including the top and bottom trays. If two muons pass through the detector in close proximity (in the viewing plane) it is possible that only one track is seen. Two apparent tracks are regarded as two muons if there is a space of one or more tubes not flashing in two or more layers. Using these selection criteria the detector efficiency for detecting vertical muons was found to be 98·8%.

It is important to know the spatial resolution of the detector when measuring particle densities. To find this resolution a distribution of the spacing of muons observed in the detector was obtained from the experimental data and compared with simulated distributions which assumed a definite detector spatial resolution. The number of

randomly spaced muons M incident upon a detector unit during the simulations was varied from $M = 2$ to $M = 15$. At each value of M some 2000 events were simulated and the detector resolution, S, expressed as a fraction of the total width of the detector, was varied in the range $0{\cdot}006 < S < 0{\cdot}020$. The simulated and experimental distributions were compared for different numbers of detected muons and different values of S. The value $S = 0{\cdot}014 \times$ total width of the detector produced the best fit to the data based on χ^2 testing.

Using this value for the detector spatial resolution, the probability of detecting m muons from M incident muons was calculated for different values of M. Finally, a relationship between the mean number of detected muons and the most probable mean number of incident muons was established. As an example, for five detected muons the most probable mean number of incident muons, on the basis of this analysis, is 5·40.

3. Analysis of results

It is known that the uncertainty in determining the core position of an EAS generally depends upon the position of the core inside the array. In order to minimize any uncertainties in core positions of the showers in the present analysis, stringent selection criteria have been employed.

These criteria are:

(i) that the distance of the centre of a shower from the centre of the Haverah Park array should be less than 500 m.

(ii) That three of the densities recorded by the 500 m array must each have exceeded the equivalent of 15 vertical penetrating muons on the 34 m^2 detectors.

(iii) That the distance of the shower core from any of the 500 m detectors must be greater than 150 m.

This third criterion was relaxed when data from the 150 m array became available during the operating period considered by this paper. With this tight selection, probable core location errors are estimated to be better than ± 20 m.

Earlier studies of the muon component of EAS at Haverah Park have usually normalized all showers present in the analysis to one value of shower size. The problem with this technique is the isolation of the non-linear relationship between muon content and shower size from the experimental data. A preferred method is to treat separately the data within selected narrow size intervals. In the present analysis, the data have been split into five intervals of shower size. Possible errors introduced into the analysis by normalization are therefore reduced to a low level.

Showers were first divided into five zenith angle intervals (0° → 65°) and then within each of these intervals the showers were further split into five intervals of shower size. The number of showers in each of these size bins having zenith angles less than 25° (ie 'vertical' EAS) are shown in table 1. Within each shower energy/zenith angle bin, EAS falling inside equal logarithmic bins of core distance were grouped together. The total number of detected muons was then found for each bin.

The muon density (corrected for spatial resolution and zenith angle) (ρ_μ) and the mean core distance and the mean value of shower size ($\overline{\rho_{500}}$) were then calculated for each distance bin. Even within the narrow intervals of shower size ρ_{500} was found to increase slightly with increasing core distance. To prevent this effect from introducing errors into the final muon densities, the value of ρ_μ was then normalized within each narrow size interval to the ρ_{500} value corresponding to the middle of the interval. The

Table 1. Number distribution of EAS, $\theta < 25°$, as a function of shower size (ρ_{500}).

ρ_{500} vem m^{-2}	Number of showers
0·32–0·45	212
0·45–0·68	330
0·68–0·98	253
0·98–1·45	140
1·45–2·18	59

relationship $\rho_\mu \propto \rho_{500}^{0.91}$ was used for this small normalization although variations of the exponent 0·91 in the wide ration 0·8–1·0 would have negligible effect on the final muon densities.

By this method the mean muon density was calculated for different core distances within each shower size interval. These results are plotted in figures 2(*a*) and (*b*) for $\theta < 25°$. The error indicated on each muon density is purely statistical and is equal to $\rho_\mu/\sqrt{N}$ where N is the total number of muons used to obtain the density.

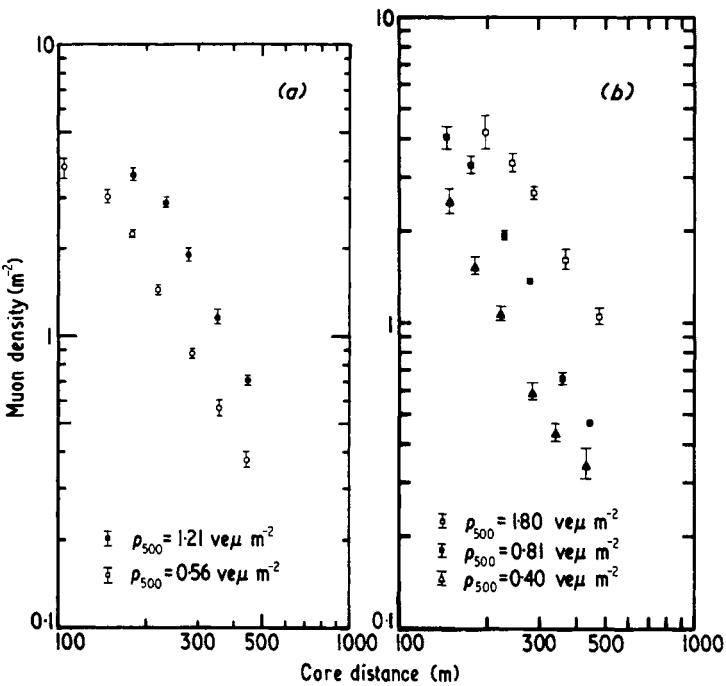

Figure 2. (*a*) and (*b*): muon density as a function of core distance and shower size.

4. The lateral density distribution of muons

The preliminary study reported by the Nottingham group (Blake *et al* 1971) used less stringent selection criteria for showers than the present analysis. In these early results

it was found that a simple power law of the form

$$\rho_\mu(\theta, R, \rho_{500}) = k(\theta)\rho_{500}^{\alpha(\theta)}R^{-n(\theta)} \tag{1}$$

could be fitted to the data. In the present analysis more rigorous selection criteria were applied to the showers contained in the analysis and the validity of the structure function of equation (1) was investigated. A function of the form $\rho_\mu \propto R^{-n}$ was fitted to the data for the five intervals of shower size for the core distance range 100 m $< R <$ 500 m and $\theta < 25°$. The values of n obtained are shown in table 2.

Table 2. The effect of fitting a simple power law, $\rho_\mu \propto R^{-n}$, over two ranges of core distance.

ρ_{500} veμ m^{-2}	R (m)	n
0·40	148–429	1·94 (±0·10)
	180–429	1·87 (±0·10)
0·56	106–448	1·73 (±0·10)
	179–448	1·95 (±0·02)
0·81	144–444	2·01 (±0·12)
	175–444	2·14 (±0·09)
1·21	180–449	1·90 (±0·12)
	234–449	2·16 (±0·02)
1·80	195–439	1·82 (±0·11)
	285–439	2·17 (±0·01)

The function was then fitted to the data in a more restricted core distance interval 200 m $< R <$ 500 m. These results together with the errors in n in fitting the points to the best straight line are also shown in table 2. Two points are evident:

(*a*) excluding the smaller values of core distance generally has the effect of increasing the slope of the structure function;

(*b*) the simple power law gives a much better fit to the data for the distance interval 200 m $< R <$ 500 m than it does for the whole interval. This is shown by the errors on n which are smaller in the restricted interval.

In order to obtain a better representation of the muon lateral distribution in the whole core distance interval a curved structure function of the type suggested by Linsley (1963) is fitted to the data. This function has the form

$$\rho_\mu \propto \frac{1}{R}\left(1+\frac{R}{R_0}\right)^{-\eta}. \tag{2}$$

The values of R_0 and η are found by using a weighted least-squares fitting process. It is found that a value $R_0 = 490$ m can be used throughout the analysis. The values of η then found for each interval of shower size are shown in table 3 together with the

probable errors in η arising in fitting the function (2) to the data. The muon lateral density distribution can therefore be represented by equation (2) where $R_0 = 490$ m and $\eta = 2{\cdot}80(\pm 0{\cdot}06)$ for 100 m $< R <$ 500 m.

Table 3. Best-fit values of structure function exponent, η, as function of shower size.

ρ_{500} veμ m^{-2}	η
0·40	2·90 (±0·07)
0·56	2·70 (±0·05)
0·81	2·90 (±0·08)
1·21	2·80 (±0·07)
1·80	2·70 (±0·04)

In order to extend the core distance interval covered, data are introduced from the Haverah Park 2 km detectors. The showers used represent a small proportion of the total number of showers recorded by the array. They have been stringently selected for inclusion in the primary energy spectrum by the Leeds University group. In this case, because of the small number of showers present, it was necessary for the muon densities to be normalized to one value of shower size to improve the statistical weight of the results.

The showers used in this analysis were first divided into zenith angle intervals as shown in table 4. Showers within the same zenith angle interval were then split into equal logarithmic bins of core distance and the muon density recorded by the flash-tube detector was then corrected for detector efficiency and resolution. Finally, the muon densities were normalized to one value of shower size, $\rho_{500} = 3{\cdot}6$, assuming $\rho_\mu \propto \rho_{500}^{0{\cdot}94}$ (see § 5).

Table 4. Number distribution of EAS used in zenith angle analysis.

Zenith angle internal (deg)	Number of EAS
$0 < \theta < 25$	229
$25 \leqslant \theta < 35$	223
$35 \leqslant \theta < 45$	322
$45 \leqslant \theta < 55$	270
$55 \leqslant \theta < 65$	180

Results for $\theta < 25°$ are plotted in figure 3. Fitting the function (2) to the data yields for $R_0 = 490$ m, $\eta = 2{\cdot}90\,(\pm 0{\cdot}17)$.

Similar analyses have been carried out for each of the zenith angle intervals up to 60°. Figure 4 plots the ratio of charged particle/muon response lateral distribution for one of the shower size intervals within each of the zenith angle intervals. The muon structure function flattens with increasing zenith angle. This flattening is illustrated by fitting function (2) to the muon data. The values of η obtained are shown in table 5.

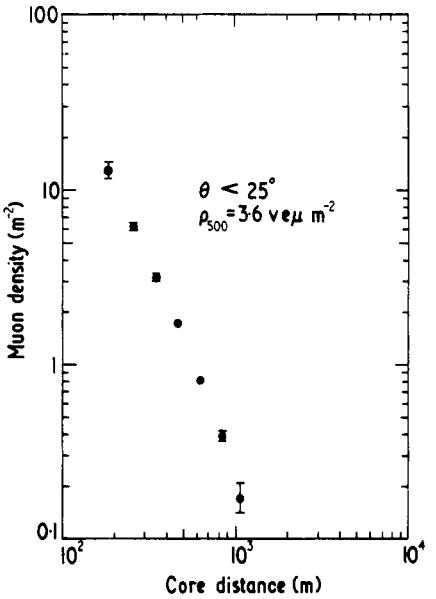

Figure 3. Muon density as a function of core distance including 2 km array showers.

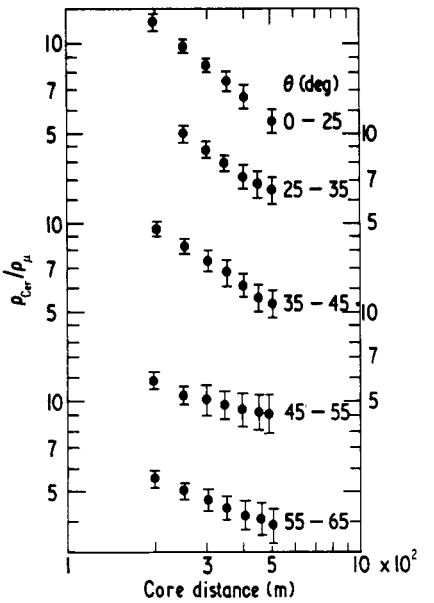

Figure 4. Ratio of charged particle to muon response as a function of core distance and zenith angle.

Table 5. Variation of η with zenith angle.

Mean zenith angle (deg)	η
17	2·80 (±0·04)
30	2·80 (±0·05)
40	2·40 (±0·14)
50	2·10 (±0·07)
60	1·40 (±0·13)

5. Variation of muon density with shower size

The variation of the muon content of EAS with ρ_{500} was carried out by fitting a function of the form

$$\rho_\mu = \frac{A}{R}\left(1+\frac{R}{490}\right)^{-\eta}$$

to the experimental data. The constant A was determined for each ρ_{500} interval. Assuming a relation of the form $\rho_\mu \propto \rho_{500}^{\alpha}$, the best-fit value of the exponent $\alpha = 0{\cdot}94$.

6. Comparison with cascade models

Hillas *et al* (1971) have computed from several different EAS models the muon and Čerenkov tank signal lateral density distribution functions for near vertical EAS. The

muon densities are calculated for the energy threshold of the present experiment, hence direct comparison of the experimental results with the model calculations is possible. The simulations differ in the models for nuclear interactions but all have the same propagation model. All the models are of a diffusion type and do not take account of any fluctuations in the development of EAS. For EAS produced by a primary mass $A > 1$ the models use a superposition treatment for the shower. The main features of the individual models are shown in table 6.

Table 6. Details of the eight Hillas models.

Model	A	D	E	F	H	I	J	K
Fraction going into pionization	0·44	0·44	0·44	0·44	0·44	0·29	0·29	0·29
Fraction going into isobars	0	0	0	0	0	0·15	0·15	0·15
Multiplicity law	$KE^{1/4}$	$KE^{1/4}$	$KE^{1/4}$	$KE^{1/4}$	$KE^{1/4}$ $KE^{1/2}$ for $(E > 3\,\text{TeV})$	$KE^{1/4}$	$KE^{1/4}$ $KE^{1/2}$ for $(E > 3\,\text{TeV})$	$KE^{1/4}$
Value of K	Forward and backward cone multiplicity changed	12	19	30	19	16	16	16
Comments							Maximum number of pions from baryon decay = 4 when $E_p = 10\,\text{TeV}$	Same as I but $\frac{2}{3}$ of baryon decays neutral

When comparing the predictions of EAS models with experimental data two factors can be taken into account: the first is the shape of the muon lateral density distribution, and the second is the absolute muon density at a fixed core position in a shower of a given primary energy. In order to compare the shape of the muon lateral distribution predicted by the different EAS models with that of the experimental data, the function (2) was fitted to the muon densities predicted by each of the models. The values of η so obtained are shown in table 7, together with the errors on η due to the fitting of this equation to the data. The predicted muon density at a core distance of 336 m for a shower size $\rho_{500} = 1{\cdot}0$ (vertical equivalent muons m^{-2}, to be written veμ m^{-2}) is also shown in the table, along with the experimental values of η and ρ_μ(336 m).

The agreement between the predictions and the experimental data is seen to be generally good for most of the models. More specifically however, models D and F do not give satisfactory agreement with the experimental value of η and must be rejected as too extreme.

Table 7. Predictions of Hillas models for different mass numbers.

Hillas model	η		ρ_μ (336 m)	
	$A = 1$	$A = 50$	$A = 1$	$A = 50$
A	2·70±0·06	2·60±0·05	1·41	1·63
E	2·70±0·05	2·60±0·05	1·28	1·52
D	3·20±0·07	3·10±0·07	0·77	1·01
F	2·50±0·05	2·30±0·07	1·53	1·68
H	2·60±0·04	2·60±0·04	1·55	1·69
J	2·70±0·05	2·60±0·05	1·39	1·54
I	2·70±0·05	2·70±0·05	1·16	1·41
K	2·80±0·05	2·70±0·05	0·93	1·18
Experimental	2·80±0·06		1·10	(±0·05)

The comparison of absolute muon densities for showers of fixed primary energy is perhaps not a good test of the models due to uncertainties in the precise connection between primary energy and the shower size parameter ρ_{500}. A more calculable parameter for comparing EAS models with experimental data is the ratio ρ_μ/ρ_{Cer} plotted as a function of core distance, where ρ_{Cer} is the recorded Čerenkov tank response. This ratio is, to a first approximation, independent of primary energy and contains information relating to both the muon and electron components of the shower. Figure 5 shows the prediction of this ratio for the different models with primary masses extending from $A = 1$ to $A = 50$, along with the experimental results. From this figure it would appear that models A, D and H can be excluded since they do not fit the experimental data for any reasonable primary mass. Model K would only fit with the experimental data if very heavy primary particles were assumed.

Models E, I and J, however, all give good agreement with the experimental data for the primary masses of approximately $A = 1$, 10 and 1 respectively in the core distance region 300–500 m. The experimental data suggest that the models predict too low a muon content about 200 m from the core. However, this suggestion is not statistically very significant.

7. The relation between $\rho_\mu(R)$ and primary energy

Using the experimental results present in §§ 4 and 5 the muon density at core distance R can be represented by the expression

$$\rho_\mu(R) = B\rho_{500}^{0\cdot94}\frac{1}{R}\left(1+\frac{R}{490}\right)^{-2\cdot8(\pm0\cdot06)} \tag{3}$$

From the measured ρ_μ, ρ_{500} and R values the constant B can be calculated as $1\cdot60(\pm0\cdot05)\times10^3$. To relate $\rho_\mu(R)$ to primary energy, E_p, requires the knowledge of the relationship between ρ_{500} and E_p. In the model E of Hillas, for proton primaries

$$E_p = 3\cdot87\times10^{17}\rho_{500}^{1\cdot018}\ \text{eV}. \tag{4}$$

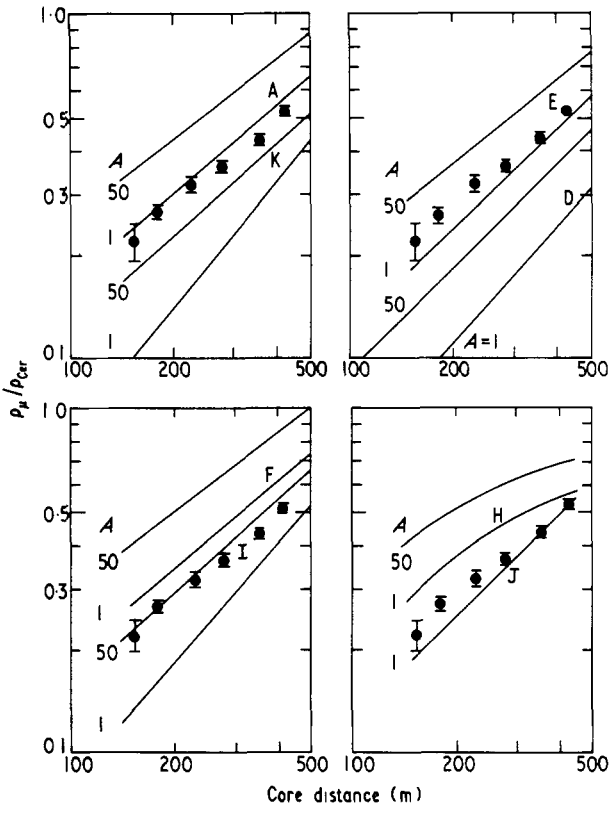

Figure 5. Ratio of muon to Čerenkov tank response as predicted by Hillas models together with experimental data.

This relationship can be derived for other Hillas models (Hillas *et al* 1971) but as stated in § 1 it is very insensitive (< 10% change) to the primary mass or acceptable variations in the nuclear model.

Combining together equations (3) and (4) yields

$$\rho_\mu(R) = 9{\cdot}2 \times 10^{-14} E_p^{0{\cdot}92} \frac{1}{R}\left(1+\frac{R}{490}\right)^{-2{\cdot}8(\pm 0{\cdot}06)} \tag{5}$$

with E_p in electronvolts and R in metres, representing the muon density lateral distribution as a function of primary energy ($10^{17} \rightarrow 10^{19}$ eV) and core distance (100 → 1000 m) for EAS with $\theta < 25°$. Using this relationship (5) between muon density (> 300 MeV) and primary energy it is hoped that a direct comparison of data from different EAS arrays can be made, and in particular the cross correlation between the muon based Sydney array and the water Čerenkov Haverah Park array.

8. Conclusions

The mean muon lateral density distribution function for EAS of primary energy about 10^{17} eV is now known to a high degree of accuracy. The study has been carried out for

both vertical and inclined showers and the results for showers at large zenith angles confirm the expected flattening of the lateral distribution.

The comparison with the EAS simulations of Hillas show that the best agreement is obtained with the more 'conservative' type model; ie that based on nuclear accelerator data. It would appear from the present results that there is no reason to suggest that nuclear interactions at these very high energies are significantly different from those covered by present day accelerator experiments.

Studies in this field are now turning to looking at the detailed distribution of fluctuations in the particle components of EAS. It is from these measurements that information should be gained which will lead to the determination of the primary mass of the cosmic rays in this primary energy range. This study is now in progress at Haverah Park.

Acknowledgments

The authors gratefully acknowledge the indispensable collaboration of all their colleagues at Haverah Park and the continuing financial support of the Science Research Council.

References

Blake P R, Ferguson H and Nash W F 1971 *Proc. 12th Int. Conf. on Cosmic Rays, Hobart* vol 3 (Hobart: University of Tasmania) pp 948–53

Hillas A M, Marsden D J, Hollows J D and Hunter H W 1971 *Proc. 12th Int. Conf. on Cosmic Rays, Hobart* vol 3 (Hobart: University of Tasmania) pp 1001–18

Linsley J 1963 *Proc. 8th Int. Conf. on Cosmic Rays, Jaipur* vol 4 (Bombay: TIFR) p 77

Wilson J G 1969 *Acta. Phys. Acad. Sci. Hung.* **29** *Suppl.* 3 409–14